

一、中文摘要

本研究對球形膠體粒子在密集的懸浮液中或在球形孔洞中於任意的外加電場下所產生的電泳現象進行數值模擬並探討。其結果可適用於任意電雙層厚度、任意表面電位且任意的外加電場強度之下，並將電雙層的極化效應與重疊效應加以考慮。我們發現若電雙層厚度在中等範圍，則表面電位高或外加電場強的情況下，求解非線性的電動力學方程式是必須的。在密集球形膠體粒子的電泳方面：當表面電位及外加電場固定時，粒子的密集度愈高則泳動度愈低。此外，當外加電場強、電雙層較厚、溶液濃度稀薄時電雙層受極化的效應均較為明顯。在球形孔洞中的電泳方面：當外加電場增大時，區域極小值會消失。當高表面電位時，電泳泳動度會隨外加電場的加大而上升。若外加電場方向向上，則與膠體粒子帶相反電性的離子會聚集於粒子的下方，且邊界的存在會影響電雙層厚度與極化效應的程度。

關鍵字：電泳現象，電雙層，泳動率。

Abstract

In this study, we investigate theoretically the electrophoresis of spherical colloids in a suspension or in a spherical cavity at arbitrary applied electric field. This analysis is applicable for arbitrary double layer thickness, surface potential and applied electric field. Moreover, the effects of double layer polarization and the overlapping are taken into account. We find that we have to solve a set of non-linear electrokinetic equations if the surface potential is high or the applied electric field is strong when the double layer thickness is in the medium range. For the case of the concentrated suspension, we conclude: For fixed surface potential and applied electric field, the higher the concentration of colloids the smaller the mobility. Moreover, the effect of double layer polarization is important if the double layer is thick, the applied electric field is strong and the concentration of suspension is low. For the case of the spherical cavity, we conclude: The local minimum of the mobility will disappear when

the applied electric field is high enough. In addition, when the surface potential is high, the mobility will increase with the increasing applied electric field. The existence of the boundary will influence the double layer thickness and the degree of double layer polarization.

Key Words : electrophoresis, double layer polarization, mobility.

二、計劃緣由與目的

The electrophoretic velocity of a charged colloid particle in an applied electric field depends on the physicochemical properties of both the particle and the liquid phase, the geometry of the system, and the magnitude of the applied electric field. A complete description of the problem under consideration involves a system of coupled partial differential equations, known as electrokinetic equations.¹ Typical assumptions made in the relevant analyses include: (1) The particle with the adjacent liquid within the shear surface is treated as a rigid sphere. (2) The properties of the liquid phase, such as density, electric conductivity, electric permittivity, and viscosity are constant, and are position independent. (3) The particle is nonconducting, and the charge on its surface distributes uniformly. (4) The classic Gouy-Chapman theory is applicable for the description of the space charge density and electric potential within the electric double layer. (5) The boundary effects are negligible, i.e., an isolated particle in an infinite electrolyte solution is considered. (6) The level of the applied electric field is low, and its effect can be simulated by considering a perturbation from the corresponding equilibrium state. In this case, the equation governing the transport of ions can be approximated by a linear expression. (7) The electrical potential of the system under consideration is low relative to the thermal energy, and the equation governing the spatial variation of electrical potential can be approximated by a linear expression. (8) The velocity of a particle is slow, and the resultant fluid flow has a negligible effect on the distributions of electrical potential and ion concentration. That is, the relaxation effects can be neglected. In general, this assumption is realistic for the case when $ka \gg 1$, where κ and a are respectively the radius of the particle and the reciprocal Debye length. Based on these assumptions Smoluchowski³ was able to derive the relation between the zeta-potential, ζ , and the electrophoretic mobility, U/E , of a particle

$$\frac{U}{E} = \frac{\varepsilon\zeta}{4\pi\eta} \quad (1)$$

where U is the electrophoretic velocity, E is the magnitude of the applied electric field, ε is the dielectric constant of the particle, and η is the viscosity of the liquid phase. Due to assumption (8), eq.(1) is not applicable for moderate values of κa . The relaxation effects were analyzed theoretically by Overbeek⁴ and Booth⁵, and they found that the deviation from eq.(1) increases with ζ . However, their quantitative validity was limited to low ζ . For the case of a general ζ , a numerical scheme is necessary. Wiersema⁶ and O'Brain⁷, for example, solved numerically the electrokinetic equations and obtained qualitatively similar results. They found that, if ζ is sufficiently high, the electrophoretic mobility has a local minimum as κa varies, and the higher the ζ , the lower the local minimum. The result of Wiersema, however, diverges at high ζ , and that of O'Brain's is restricted to assumption (6). The electrophoretic behavior of a polyion in an infinite fluid was examined recently by Allison and Nambi,⁸ the governing equations were solved by a combined DIE/finite difference algorithm. Their work was also limited to assumption (6); the same problem was also solved by a boundary element method.⁹ Allison and Nambi concluded that the accuracy of the spatial variation of electrical potential and ion density is crucial in the estimation of the electrophoretic mobility of a charged entity.

If the presence of a boundary needs to be considered, the problem becomes even more complicated. Previous results¹⁰⁻¹⁷ were limited to assumptions (1)-(8). Also, it was assumed that the equation describing the electric field could be decoupled from the hydrodynamic equation. This is applicable only if $\kappa a \rightarrow \infty$, i.e., thin double layers. Zydney¹⁸ incorporated electric forces into the hydrodynamic equation and thus his results are applicable to all κa , but both the relaxation effects and the distortion of ion cloud under the applied field were neglected. Zydney¹⁸ evaluated the electrophoresis of a sphere at the center of a spherical cavity, and under the condition of low surface potential, the essentially one-dimensional problem was solved analytically. Although the geometry considered is an idealized one it is capable of providing insights in the electrophoretic behaviors of a colloid particle in porous media. The simple geometry was also adopted to simulate a concentrated colloidal dispersion.¹⁹⁻²³ Lee et al.²⁴⁻²⁶ extended the analysis of Zydney by taking the relaxation effects and double layer polarization into account. They showed that, similar to the case of an infinite fluid, if the surface potential is sufficiently high, the electrophoretic mobility has a local minimum as κa varies. Although

assumptions (7) and (8) were eliminated in their study, the results of Lee et al.²⁴⁻²⁶ were limited to assumption (6).

If assumption (6) is applicable, the equation describing the transport of ions can be approximated by a linear expression. This implies that the magnitude of the applied electrical field will not affect the distribution of scaled mobility. In this case, the electrokinetic equations become linear, and the problem under consideration can be divided into two sub-problems, which implies that tedious iterations can be avoided in the calculation of the electrophoretic mobility.^{7,24-26} In practice, however, since the magnitude of the electric field can have a significant effect on the spatial distribution of the scaled variables, a more general treatment is highly desirable. This is done in the present. Here, a pseudo-spectral numerical scheme is used to solve the general electrokinetic equations for the case when a boundary is present. For illustration, the geometry of Zydney¹⁸ is adopted and the nonlinear effects of the magnitude of the applied field are analyzed.

三、研究方法和成果

Referring to Fig.1, we consider a rigid, non-conducting sphere of radius a at the center of a non-conducting spherical cavity of radius b . A uniform electric field E is applied in the z -direction. The spherical coordinates (r, θ, ϕ) with its origin located at the center of the cavity are adopted. The electrokinetic equations include that for the conservation of ions, that for the electrical potential, and the hydrodynamic equations. The conservation of ions leads to

$$\frac{\partial n_j}{\partial t} = \bar{\nabla} \cdot \left\{ D_j \left[\bar{\nabla} n_j + \frac{z_j e n_j}{k_B T} \bar{\nabla} \phi \right] + n_j \bar{v} \right\} \quad (2)$$

where $\bar{\nabla}$ is the gradient operator, n_j , D_j , and z_j are respectively the number concentration, the diffusivity, and the valence of ionic species j , e is the elementary charge, ϕ is the electric potential, \bar{v} is the fluid velocity, and k_B and T are respectively the Boltzmann constant and the absolute temperature. We assume that the electrical potential can be described by the Poisson equation

$$\bar{\nabla}^2 \phi = -\frac{\rho}{\varepsilon} = -\sum_{j=1}^M \frac{z_j e n_j}{\varepsilon} \quad (3)$$

where ε is the permittivity of the liquid phase, ρ is the space charge density, and M is the total number of ionic species.

Suppose that the flow field around the sphere can be described by the Navier-Stokes equations in the creeping flow regime with electrical body forces considered. We have

$$\bar{\nabla} \cdot \bar{v} = 0 \quad (4)$$

$$\rho_f \frac{\partial \bar{v}}{\partial t} = \eta \nabla^2 \bar{v} - \bar{\nabla} p - \rho \bar{\nabla} \phi \quad (5)$$

In these expressions p is the pressure, and ρ_f and η are the fluid density and viscosity respectively. We assume that the motion of the particle is slow so that the system is at a quasi-steady state, and the terms that involve the time derivative in the governing equations can be neglected.

四、結果與討論

Figure 2 shows the variation of scaled mobility U_m^* as a function of κa at various levels of scaled applied field E_z for the case of low surface potential, the corresponding results for higher surface potentials are presented in Figs.3 and 4.

As pointed out by Chu et al.²⁴⁻²⁶, if the surface potential is low, the electric field can be described satisfactorily by a linearized Poisson-Boltzmann equation. As suggested by Fig.2, if the surface potential is sufficiently low, using the linearized Poisson-Boltzmann equation is appropriate regardless of the level of E_z . Figures 3 and 4 reveal that, however, as ϕ_r becomes appreciable, both the quantitative and the qualitative behaviors of $U_m^* - \kappa a$ curve based the linearized Poisson-Boltzmann equation (linear model) and those based on the original nonlinear Poisson-Boltzmann equation (nonlinear model) are different. For example, Fig.3 shows that if E_z is low (linear model is applicable), U_m^* exhibits a local minimum as κa varies. This local minimum vanishes if E_z is sufficiently high. Also, the deviation of nonlinear model from the corresponding linear model increases with the level of E_z . On the other hand, if $\kappa a \rightarrow 0$, both linear model and nonlinear model lead to the same U_m^* regardless of the levels of ϕ_r and E_z , as can be seen from Figs.2 through 4. The disappearance of the local minimum of $U_m^* - \kappa a$ curve if E_z is high can be explained by the behavior of K_E as κa varies. According to eqs.(29) and (30), K_E is a measure for the

contribution to electrophoretic mobility by the electrostatic force. In eq.(29), $(\partial \phi_1^* / \partial r^*)_{r^*=1}$ increases with κa , but the reverse is true for $(\partial \phi_2^* / \partial \theta^*)_{r^*=1}$. This is because the larger the κa , the faster the spatial variation of electrical potential in the double layer, i.e., the larger the $-\nabla^* \phi_1^*$. This has the effect of reducing the influence of the applied electric field. The variation of $2K_E$ as a function of κa at various levels of scaled applied field E_z for the case $\phi_r = 3$ is presented in Fig.5, and that for a higher ϕ_r is shown in Fig.6. These figures reveal that if E_z is low, K_E has a local minimum as κa varies, and the higher the ϕ_r , the more pronounced the local minimum. However, if K_E is sufficiently high, the local minimum disappears. This is because if E_z is low, K_E is dominated by $(\partial \phi_1^* / \partial r^*)_{r^*=1}$, and it is dominated by $(\partial \phi_2^* / \partial \theta^*)_{r^*=1}$ if E_z is high.

Figures 7 through 10 illustrate the contours for the net scaled ion concentrations CD defined as $(n_1^* - n_2^*)$ for various combinations of κa and E_z . Since the particle is positively charged, CD is negative. Figure 7 shows that if E_z is low, the contour is circular even if the double layer is thick, that is, double-layer polarization is insignificant. This is expected since the velocity of the particle is small. Figure 8 suggests that if double layer is thin, its polarization is also insignificant even if the applied electric field is appreciable. As stated previously, this is because $-(\partial \phi_1^* / \partial r^*)_{r^*=1}$ increases with κa , which has the effect of reducing the influence of the applied electric field. Double-layer polarization becomes significant, however, if E_z is sufficiently high or

the double layer is sufficiently thick, as suggested by Figs.9 and 10. These figures reveal that the concentration of anions at the bottom of a particle is higher than that at the top of the particle, that is, anions are concentrated on the bottom of the particle. This is because the movement of the particle is in the direction pointing toward the top of the particle.

Figures 11 through 13 simulate the effect of the presence of a boundary on the electrophoretic behavior of a particle. The variation of scaled mobility U_m^* as a function of ka at various $\lambda (=a/b)$ is shown in Fig.11. Figures 12 through 13 illustrate the contours for the net scaled ion concentrations CD defined as $(n_1^* - n_2^*)$ for various combinations of ka and λ . Figure 11 shows that for fixed surface potential and applied electric field, the electrophoretic mobility of a particle decreases with the increase in λ . That is, the closer the particle to the cavity wall the smaller the mobility. Apparently, the flow field is influenced by the presence of the boundary, which has the effect of reducing the terminal velocity of the particle. The presence of the boundary will also affect the variation in the thickness of double layer, and the degree of double-layer polarization. A comparison between Figs.8 and 12, for example, reveals the former where the rate of decrease in the thickness of double layer is slower if λ is larger. As can be seen in Fig.13, if double layer is thick and λ is small, the effect of the top and the bottom parts of the cavity wall on CD is more significant than that of the left and the right parts of the cavity wall. This leads to the elliptical-shaped contour near cavity wall. This may be due to the fact that the movement of the particle is in the direction from the bottom to the top.

五、参考文献

1. Hunter, R.J., in "Foundations of Colloid Science." Vols. I and II, Clarendon Press, Oxford, 1989.
2. Smoluchowski, M., *Z. Phys. Chem.*, **92**, 129 (1918).

3. Dukhin, S.S., and Derjaguin, B.V., in "Surface and Colloid Science." Vol.7, Wiley, New York, 1974.
4. Overbeek, J. Th. G., *Advan. Colloid Sci.* **3**, 97 (1950).
5. Booth, F., *Proc. Roy. Soc. Lond. A*, **203** 514 (1950).
6. Wiersema, P.H., Loeb, A.L., and Overbeek, J.Th.G., *J. Colloid Interface Sci.*, **22**, 78, (1966).
7. O'Brien, R.W., and White, L.R., *J. Chem. Soc. Faraday II.*, **74**, 1607 (1978).
8. Wiersema, P.H., Loeb, A.L., and Overbeek, J.Th.G., *J. Colloid Interface Sci.*, **22**, 78, (1966).
9. O'Brien, R.W., and White, L.R., *J. Chem. Soc. Faraday II.*, **74**, 1607 (1978).
10. Jorgenson, J.W., *Anal. Chem.*, **58**, 743A (1986).
11. Keh, H.J., and Anderson, J.L., *J. Fluid Mech.*, **153**, 417 (1985).
12. Keh, H.J., and Chiou, J.Y., *Am. Inst. Chem. Eng. J.*, **42**, 1397 (1996).
13. Morrison, F.A., and Stuhel, J.J., *J. Colloid Interface Sci.*, **33**, 88 (1970).
14. Keh, H.J., and Chen, S.B., *J. Fluid Mech.*, **194**, 377 (1988).
15. Keh, H.J., and Lien, L.C., *J. Fluid Mech.*, **224**, 305 (1991).
16. Keh, H.J., Horng, K.D., and Kuo, J., *J. Fluid Mech.*, **231**, 211 (1991).
17. Feng, J.J., and Wu, W.I., *J. Fluid Mech.*, **264**, 41 (1994).
18. Zydney, A.L., *J. Colloid Interface Sci.*, **169**, 476 (1995).
19. Levine, S., and Neale, G.H., *J. Colloid Interface Sci.*, **47**, 520 (1974).
20. Kozak, M.W., and Davis, E.J., *J. Colloid Interface Sci.*, **112**, 403 (1986).
21. Kozak, M.W., and Davis, E.J., *J. Colloid Interface Sci.*, **127**, 497 (1989).
22. Kozak, M.W., and Davis, E.J., *J. Colloid Interface Sci.*, **129**, 166 (1989).
23. Ohshima, H., *J. Colloid Interface Sci.*, **188**, 481 (1997).
24. E. Lee, J.W. Chu, and J.P. Hsu, *J.P. J. Colloid Interface Sci.* **196**, 316 (1997)
25. E. Lee, J.W. Chu, and J.P. Hsu, *J.P. J. Colloid Interface Sci.* **205**, 65 (1998)
26. E. Lee, J.W. Chu, and J.P. Hsu, *J.P. J. Colloid Interface Sci.* **209**, 240 (1999)

Fig.1. Schematic representation of the system where a sphere of radius a is placed at the center of a spherical cavity of radius b .

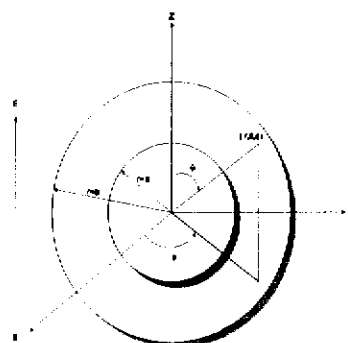


Fig.2. Variation of U_m^* as a function of ka at various

levels of scaled applied field E_z^* for the case the sphere is positively charged with $\phi_r=1$ and the cavity uncharged. Key: $\lambda=0.5, \alpha=1$, and $Pe_1=Pe_2=0.01$.

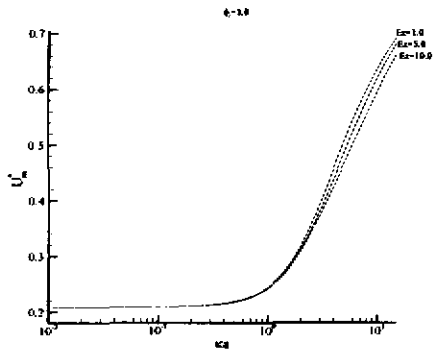


Fig.3. Variation of scaled mobility U_m^* as a function of $\kappa\alpha$ at various levels of scaled applied field E_z^* for the case $\phi_r=3$. Key: same as Fig.2.

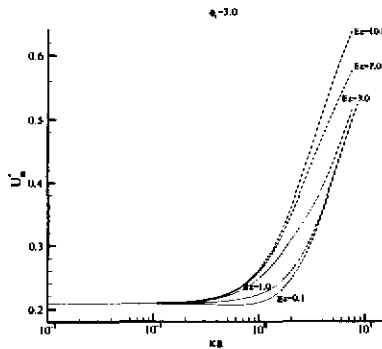


Fig.4. Variation of scaled mobility U_m^* as a function of $\kappa\alpha$ at various levels of scaled applied field E_z^* for the case $\phi_r=5$. Key: same as Fig.2.

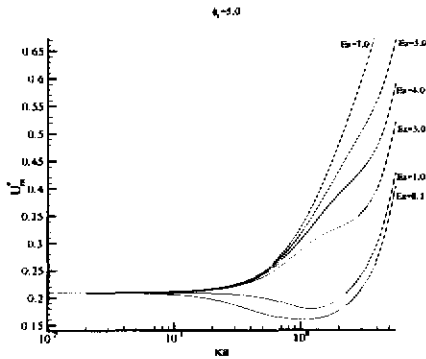


Fig.5. Variation of $2K_E$ as a function of $\kappa\alpha$ at various levels of scaled applied field E_z^* for the case $\phi_r=3$. Key: same as Fig.2.

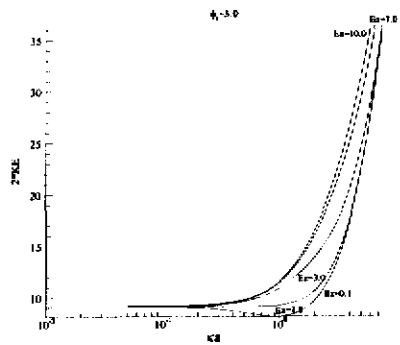


Fig.6. Variation of $2K_E$ as a function of $\kappa\alpha$ at various

levels of scaled applied field E_z^* for the case $\phi_r=5$. Key: same as Fig.2.

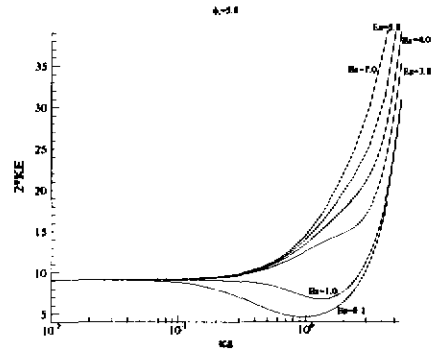


Fig.7. Contours for the net scaled ion concentrations $CD (=n_1^- - n_2^-)$ for the case $\phi_r=3, \kappa\alpha=0.01, \lambda=0.5, E_z^*=0.01, Pe_1=Pe_2=0.01$, and $\alpha=1$.

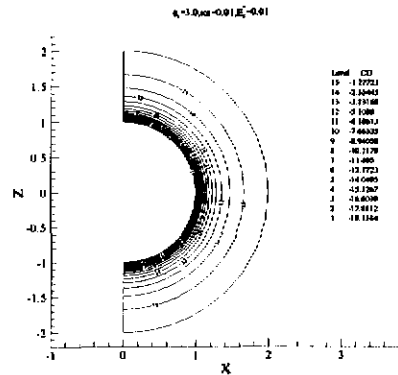


Fig.8. Contours for the net scaled ion concentrations $CD (=n_1^- - n_2^-)$ for the case $\phi_r=3, \kappa\alpha=5.6, \lambda=0.5, E_z^*=1, Pe_1=Pe_2=0.01$, and $\alpha=1$.

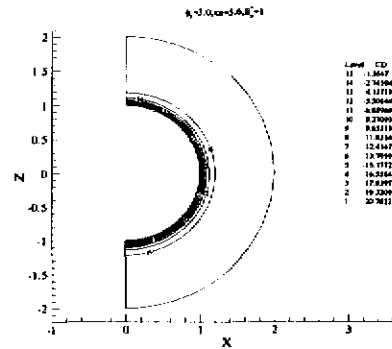


Fig.9. Contours for the net scaled ion concentrations $CD (=n_1^- - n_2^-)$ for the case $\phi_r=3, \kappa\alpha=0.01, \lambda=0.5, E_z^*=1, Pe_1=Pe_2=0.01$, and $\alpha=1$.

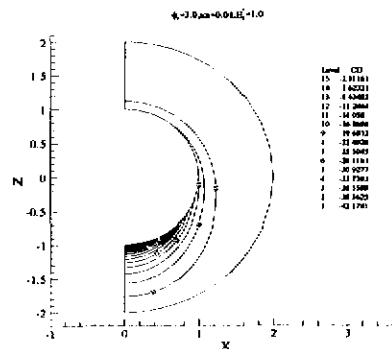


Fig.10. Contours for the net scaled ion concentrations CD

($=n_1 - n_2$) for the case $\phi_r=3$, $\kappa\alpha=0.01$, $\lambda=0.5$, $E_z=5$, $Pe_1=Pe_2=0.1$, and $\alpha=1$.

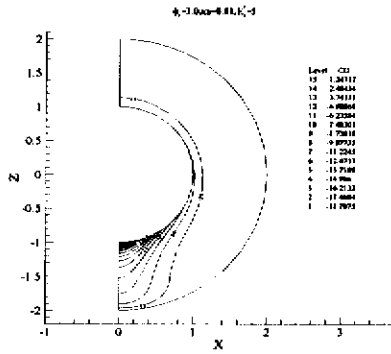


Fig.11. Variation of scaled mobility U_m as a function of $\kappa\alpha$ at various $\lambda (=a/b)$ for the case $\phi_r=1$, $E_z=3$, $Pe_1=Pe_2=0.01$, and $\alpha=1$.

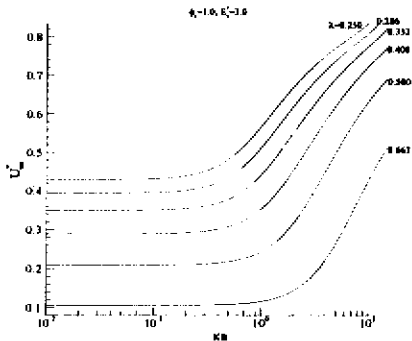


Fig.12. Contours for the net scaled ion concentrations CD ($=n_1 - n_2$) for the case $\phi_r=1$, $\kappa\alpha=5.6$, $\lambda=0.667$, $E_z=3$, $Pe_1=Pe_2=0.01$, and $\alpha=1$.

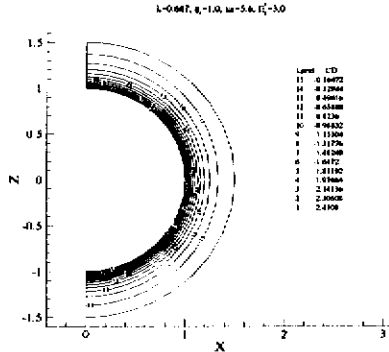


Fig.13. Contours for the net scaled ion concentrations CD ($=n_1 - n_2$) for the case $\phi_r=1$, $\kappa\alpha=0.01$, $\lambda=0.25$, $E_z=3$, $Pe_1=Pe_2=0.01$, and $\alpha=1$.

